Improved survival in a long term rat model of sepsis is associated with reduced mitochondrtial calcium uptake despite increased energetic demand?

Bernardo B. Pinto, MD PhD[1,2,3],

Alex Dyson, PhD[1],

Michele Umbrello, MD[1,4],

Jane E. Carré, PhD[1],

Cristiane Ritter, MD PhD[1,5],

Innes Clatworthy, PhD[6],

Michael R. Duchen, PhD, FRCP [7],

Mervyn Singer, MD FRCP[1]

1. Bloomsbury Institute of Intensive Care Medicine, Division of Medicine, University College London, London, UK (where the work was performed); 2. Department of Anaesthesia, Emergency and Intensive Care, Centro Hospitalar do Porto, Porto, Portugal; 3. Department of Pharmacology, Anaesthesia and Intensive Care, Geneva University Hospitals, Geneva, Switzerland; 4. Dipartimento di Fisiopatologia Medico-Chirurgica e dei Trapianti, Università degli Studi di Milano, Milan, Italy; 5. Laboratório de Fisiopatologia Experimental, Universidade do Extremo Sul Catarinense, Criciúma, SC, Brazil; 6. Electron Microscopy Unit, Royal Free Hospital, London, UK; 7. Department of Cell and Developmental Biology, University College London, UK.

Correspondence to: Bernardo Bollen Pinto

Geneva University Hospitals, Department of Anaesthesia, Intensive Care and Pharmacology, Rue Gabrielle-Perret-Gentil 4, 1205 Geneva, Switzerland.

bernardo.bollenpinto@hcuge.ch

Financial support statement: Bernardo Bollen Pinto was supported by a Portuguese Science Foundation PhD scholarship through the Graduate Program in the Areas of Basic and Applied Biology (GABBA) of Porto University (SFRH / BD / 33540 / 2008). MS is a Senior Investigator of the UK National Institute of Health Research (NIHR). UCLH/UCL receives a proportion of funding from the UK Department of Health's NIHR Biomedical Research funding scheme.

Key words: sepsis, heart, myocardial depression, mitochondria, efficiency.

Abstract

Objective: To investigate the relationship between prognosis, changes in mitochondrial calcium uptake and bioenergetic status in the heart during sepsis.

Design: *In vivo* and *ex vivo* controlled experimental studies.

Setting: University research laboratory.

Subjects: Male adult Wistar rats.

Interventions: Sepsis was induced by intraperitoneal injection of fecal slurry. Sham-operated animals served as controls. Confocal microscopy was used to study functional and bioenergetic parameters in cardiomycoytes isolated after 24 h sepsis. Electron microscopy (EM) was used to characterize structural changes in mitochondria and sarcoplasmic reticulum. The functional response to dobutamine was assessed *in vivo* by echocardiography.

Measurements and main results: Peak aortic blood flow velocity measured at 24 h was a good discriminator for 72 h survival (AUROC 0.84±0.1, p=0.03) and was used in *ex vivo* experiments at 24 h to identify septic animals with good prognosis. Measurements from animals with good prognostic showed i) a smaller increase in mitochondrial calcium content and in NADH fluorescence following pacing and ii) increased distance between mitochondria and SR on EM, and iii) NADH redox potential and ATP/ADP failed to reach a new steady state following pacing, suggesting impaired matching of energy supply and demand. *In vivo*, good prognosis animals had a blunted response to dobutamine with respect to stroke volume and kinetic energy.

Conclusions: In situations of higher energetic demand decreased mitochondrial calcium uptake may constitute an adaptive cellular response that confers a survival advantage in response to sepsis at a cost of decreased oxidative capacity.

Introduction

Myocardial depression is a well-recognized phenomenon in patients with septic shock with reported incidence rates of 40-50% (1,2). The underlying pathophysiology is complex with multiple factors implicated (3,4). We (5-7) and others (8-10) reported derangements in energetic status and have proposed that impaired energy homeostasis may be an important contributory factor to organ dysfunction in sepsis. Findings in rodent endotoxic shock models include depressed myocardial ATP levels or reduced activity of mitochondrial respiratory complexes (11,12). Studies using more clinically relevant models of polymicrobial sepsis report variable degrees of myocardial and mitochondrial dysfunction, often with unchanged levels of phosphate intermediates (13-15). Myocardial dysfunction in sepsis may be the result of a hibernation-like state, whereby cardiomyocytes decrease mitochondrial oxygen consumption under conditions of lower cellular metabolic demand (2,3). However, this notion remains to be confirmed as most studies have only used steady state measures of mitochondrial function, rather than capturing the interaction between energy supply and demand.

Long before modern bioenergetic theory Starling postulated a linear relationship between oxygen consumption and cardiac work (16). Phosphorylation potential (i.e. [ATP]/[ADP].[Pi]) is a primary regulator of mitochondrial ATP production (17). Under conditions of high energetic demand, such as those seen in the heart in response to an increased workload or acute stress (as in sepsis), a rise in cytosolic calcium is accompanied by a rise in intramitochondrial calcium content mediated by

mitochondrial calcium uptake pathways. Furthermore, stimulation of mitochondrial oxidative phosphorylation by calcium increases ATP production to match an increase in demand (18,19). However, if mitochondrial calcium levels increase above a certain threshold, mitochondrial calcium overload can result in cell death via opening of the mitochondrial permeability transition pore (20).

The presence of myocardial depression, defined echocardiograpically (21-25) or by elevations in cardiac injury/dysfunction biomarkers such as troponin or B-type natriuretic peptide (26-28), is strongly associated with an increased mortality risk in septic patients. An important limitation in experimental studies proposing a role for mitochondria in septic cardiomyopathy is that they fail to consider the heterogeneity observed in human populations where patients may/may not develop septic cardiomyopathy. We thus sought to use our fluid-resuscitated rat model of fecal peritonitis, where early (at 6 or 24 h post-insult) differences in systolic function can predict 3-day mortality (29,30), to investigate the effect of sepsis on the energetic response of the heart *in vivo* to an increase in metabolic activity in a cohort of rodents identified with positive prognostic indicators. In addition, we aim to associate these responses with those of bioenergetically relevant intermediates at the cellular level, including mitochondrial calcium, mitochondrial NADH, ATP/ADP and mitochondrial membrane potential. Using electron microscopy we also examined the proximity of mitochondria to sarcoplasmic reticulum as this may affect the degree of calcium release (31).

Materials and methods

Rat model of fecal peritonitis

Male Wistar rats (12-14 weeks old) were used in all *in vivo* and *ex vivo* studies. All experiments were performed according to local ethics committee (University College London) and Home Office (UK) guidelines under the 1986 Scientific Procedures Act. This model has been described in detail elsewhere (30). In brief, anesthetized rats underwent right jugular vein and left carotid artery cannulation. These catheters were tunneled subcutaneously and mounted onto a swivel-tether system (Instech, Plymouth Meeting, PA) allowing the animal unimpeded movement in its cage, free access to food and water, intravenous fluid administration and blood pressure monitoring. After overnight recovery, sepsis was induced by an intraperitoneal injection of fecal slurry (32). Sham animals (control) received an equivalent volume of 0.9% saline. Two hours post-injection of slurry/saline, a continuous intravenous infusion of glucose and 6% hydroxyethyl starch 130/0.4 (Volulyte, Fresenius Kabi, Bad Homburg, Germany) (1:1) was started at 10 ml/kg/h and halved at 24 h intervals. A validated clinical scoring system was used to assess overall disease severity (33). Supplemental Digital Content 1 shows the main characteristics of the study cohorts, and Supplemental Digital Content 2 further details on the model.

Echocardiography measurements

Echocardiography was performed to measure stroke volume (34), peak blood flow velocity (a measure of left ventricular contractility) (35) and kinetic energy (36). Further details can be found in Supplemental Digital Content 2.

Serum assays

An arterial blood sample of 0.7 ml was withdrawn at 6 and 24 h post-insult for blood gas analysis (ABL 800 Flex Analyzer, Radiometer, Copenhagen, Denmark) and collection of plasma for subsequent batch analysis of interleukin (IL-) 6 and 10 (Rat-Quantikine enzyme-linked immunosorbent assay kits, R&D Systems, Wiesbaden, Germany).

Confocal microscopy

Non-permeabilized adult rat ventricular myocytes isolated from septic animals and sham controls by conventional enzymatic dissociation (37,38) were plated on laminin-coated coverslips and imaged using a Zeiss 510 CLSM META confocal microscope. TMRM was used as a measure of mitochondrial membrane potential, NADH autofluorescence of redox state, Fluo-4 acetoxymethyl AM and Rhod-2 AM to measure changes in cytosolic and mitochondrial calcium, respectively. Magnesium Green fluorescence was used as a relative indicator of the ATP/ADP ratio (39). Further details can be found in Supplemental Digital Content 2.

Electron microscopy

Left ventricle samples were obtained for structural analysis by electron microscopy. Further details can be found in Supplemental Digital Content 2. For each tissue sample, ten imaging areas were defined as regions where intermyofibrillar mitochondria could be clearly identified among longitudinally-oriented myofibrils, in close proximity to the sarcoplasmic reticulum (junctional SR, jSR) (31). As several of the mitochondrial citric acid cycle dehydrogenases are stimulated by calcium, we hypothesized that proximity

of jSR to the intermyofibrillar mitochondria could affect the rate and efficiency of NADH oxidation and ATP production in sepsis.

Data analysis and statistical procedures

All datasets were tested for normality of distribution using the Kolmogorov-Smirnov test. Normally distributed data were compared using Student's t test or analysis of variance (one-way or two-way ANOVA with repeated measures, as appropriate). If appropriate, post-hoc testing was performed using a Bonferroni correction. Results were expressed as mean ± SEM. Non-parametric data were compared using the appropriate equivalent, and expressed as median and interquartile range. Differences in survival were analysed with the log-rank test. The quality of echocardiography-derived measurements as a prognostic test was described by the area under the Receiver operator characteristic (AUROC) curve. All analyses were performed using IBM SPSS Statistics, Version 22.0 (IBM Corp, Armonk, NY) and graphs built using Prism Version 6.0 (GraphPad Software, La Jolla, CA). Probability values <0.05 were considered statistically significant.

Results

Model characterization and identification of animals with good prognosis

For survival studies, 4 sham and 12 septic animals (Cohort 1) were followed for 72 h. All sham animals survived while 9 (75%) of the septic animals died (Figure 1). Clinical severity, blood pressure and biochemical measures of arterial blood oxygenation, metabolism and inflammation can be found in the Supplemental Digital Content 3. Animals still alive at 72 h showed evidence of clinical recovery with increased interest and activity in their environment. In this model, sepsis was not associated with hypotension nor hypoglycemia due to ongoing fluid resuscitation and glucose infusion.

In further experiments, 8 sham and 22 septic rats (Cohort 2) were followed for up to 72 h with echocardiography performed under a short period of light anesthesia at 6, 24 and 72 h post-insult. Septic non-survivors showed depressed cardiac contractility (peak velocity), stroke volume and cardiac output, as early as 6 h post-injection of fecal slurry (Table 1). Kinetic energy (KE), an *in vivo* measure of the work developed by the left ventricle, was also significantly depressed (Table 1). In order to classify animals according to disease severity in terminal experiments performed at 24 h post-insult, we tested the ability of selected cardiac and clinical variables to predict 72 h survival (Supplemental Digital Content 4). An aortic blood flow peak velocity cut-off of 0.93 m/s measured at 24 h could distinguish septic animals into good and bad prognosis groups (AUROC 0.84±0.1, p=0.03) and was used in terminal experiments to separate septic animals into good and poor prognosis groups.

Mitochondrial calcium uptake and NADH fluorescence in isolated cardiomyocytes

In a separate cohort of animals, 4 sham and 8 septic rats (Cohort 3) were randomized for *ex vivo* confocal microscopy studies of intact, isolated cardiomyocytes at 24 h post-insult. Mortality in the septic group was 50%. All surviving animals had an aortic flow peak velocity >0.93 m/s, suggesting a good prognosis.

Baseline NADH and TMRM fluorescence were significantly lower in resting septic cardiomyocytes isolated from good prognosis animals compared to sham (Figures 2A,B). Using a physiologically relevant model of increased energy demand, we observed that mitochondrial calcium (Rhod2 fluorescence, Figure 2C) increased as expected (40) with electrical pacing in both sham and septic cells. However, the rise was significantly attenuated in septic cardiomyocytes from good prognosis animals. Importantly, these differences were unlikely to be due to changes in total calcium as the Fluo4 signal was similar between sepsis and control cardiomyocytes (Figure 2D).

Figure 2E illustrates two representative traces of MgGreen fluorescence in septic and control cardiomyocytes. After steady-state measurements at rest (a,a'), pacing-induced contraction caused an increase in MgGreen fluorescence. This likely reflects a decreased ATP:ADP ratio, with the dissociation of free Mg^{2+} from ADP following ATP hydrolysis (b,b'). Establishment of a new equilibrium between ATP production and hydrolysis was inferred in all sham cardiomyocytes with MgGreen fluorescence stabilizing or returning to pre-stimulation levels (c) within 30 seconds after pacing (n=6/6). However, only half of the septic cardiomyocytes reached a new steady state with the others presenting a continuous increase in MgGreen fluorescence (c') (n=3/6), suggesting net ATP hydrolysis. We also investigated the response of MgGreen

fluorescence in sham and septic cells to combined inhibition of glycolysis and oxidative phosphorylation using 2-deoxyglucose and oligomycin, respectively. Most of the sham cells (n=3/5) reached a new steady state fluorescence as illustrated in Figure 5D (d). Only one septic cardiomyocyte reached a new steady state (d') with the remaining showing gradually increasing MgGreen fluorescence (n=4/5) until the addition of the mitochondrial uncoupler, FCCP that resulted in depletion of cellular ATP.

After observing derangements in the two main mechanisms that relate sarcoplasmic energetic needs to the mitochondria (calcium and ATP/ADP ratio) we studied changes in mitochondrial NADH redox status in response to pacing. The initial response upon stimulation of contraction was an increase in NADH autofluorescence indicating an increase in reduced NADH (Figure 2F). This is likely due at least in part, to calcium-induced stimulation of mitochondrial TCA cycle dehydrogenases (18). Cardiomyocytes from septic animals presented a smaller peak increase compared to sham (9.9 vs. 3.7%, $p<0.05$). Following the initial rise, in sham cardiomyocytes NADH autofluorescence returned to a steady state similar to baseline levels, i.e. redox homeostasis was re-established. In septic cells, a steady state was not achieved following pacing (Figure 2F): NADH autofluorescence continued to decline, representing net NADH oxidation.

Structural relationship between mitochondria and junctional sarcoplasmic reticulum

The majority of the mitochondrial calcium signal originates in the jSR. To investigate whether the distance between these organelles could explain the attenuated pacing-induced rise in mitochondrial calcium, a further cohort of fifteen rats was randomized

to sham (n=5) and sepsis (n=10) (Cohort 4) for electron microscopy studies. Two septic animals died before reaching the 24 h timepoint. Five of the eight remaining animals were classified as 'good prognosis' (i.e. peak velocity >0.93 m/sec) at 24 h.

Intermyofibrillar mitochondria from the left ventricle of good prognosis septic animals had a smaller transversal side length (Figure 3). This is the area that develops preferential contact with jSR and hence is more prone to acute changes in calcium. The distance between the mitochondrial outer membrane and the jSR was greater in septic cardiomyocytes (Figure 3). Importantly, these observations were not due to differences in mitochondrial density or shape (Supplemental Digital Content 5).

In vivo response to increased energetic demand

At rest, systolic function was similar between septic rats with good prognosis and sham controls (Table 1). To clarify whether the phenotype identified *ex vivo* suggesting derangements in sarcoplasmic-mitochondria communication had *in vivo* functional translation, echocardiography was performed before and after infusion of a positive inotrope (dobutamine). Both the inotropic and KE response to dobutamine at 24 h was depressed in septic animals with good prognosis compared to sham controls (Figure 4).

Discussion

Reduced ATP supply from dysfunctional mitochondria has been proposed as a mechanism underlying septic cardiomyopathy (41). However, most of the available evidence originates from measurements of phosphate intermediates or biochemical assays of respiratory complex activity. Mitochondrial function needs to be assessed under different energetic loads to determine whether a dysfunction really exists. We investigated the response of different bioenergetically relevant parameters to changes in ATP demand in hearts *in vivo*, and in intact, non-permeabilized cardiomyocytes. As we wished to understand mechanisms associated with survival in the context of septic cardiomyopathy, we focused our studies on a selected subgroup of septic rats with good 3-day survival.

In this group of septic animals with good prognosis we observed (i) a lesser increase in mitochondrial calcium uptake upon electrical pacing that was associated with (ii) a greater distance between mitochondria and junctional sarcoplasmic reticulum. Functionally, (iii) a blunted NADH peak fluorescence and delayed steady state response to pacing suggests an inadequate response of citric acid cycle dehydrogenases to calcium. This could help explain (iv) the blunted response to dobutamine observed *in vivo* in terms of stroke volume and kinetic energy.

Oxidation of the mitochondrial NADH (and FAD) pool by the electron transport chain generates a proton gradient across the inner mitochondrial membrane that is then used by ATP synthase to phosphorylate ADP (17). In the initial response to electrical stimulation (a physiologically relevant form of increased ATP demand), septic cardiomyocytes reduced the NADH pool to a lesser extent than controls.

Notably, sham though not septic cardiomyocytes could re-establish homeostasis of their mitochondrial redox potential, as evidenced by achieving a new steady state of NADH fluorescence. Taken together, these findings suggest a mismatch in the rates of one or more processes that contribute to mitochondrial NADH redox state homeostasis, e.g. the relative bound-to-free NADH ratio, metabolite shuttle activity or NADH oxidation:reducing activity, in septic cardiomyocytes. Notwithstanding the difference in baseline NADH autofluorescence, when combined with the smaller initial rise in NADH autofluorescence signal seen on pacing, our findings indicate a potentially inadequate response of citric acid cycle dehydrogenases to an increase in demand for ATP in sepsis. Septic cardiomyocytes also largely failed to reach a steady state ATP:ADP ratio after pacing-induced contraction. Although MgGreen fluorescence is not a direct measurement of ATP concentration or flux, our data suggest differences in the way that the ATP:ADP ratio responds to changes in energy demand in cardiomyocytes isolated from sham and septic animals.

Septic cardiomyocytes presented decreased TMRM fluorescence at rest, indicating a lower mitochondrial membrane potential, that has been previously reported in adult rat atrial myocytes in polymicrobial sepsis (42) and in adult ventricular myocytes following endotoxemia (43), but mechanisms and impact remained unexplained. A low mitochondrial membrane potential could impact on our mitochondrial calcium observations, as membrane potential is an important driving force of mitochondrial calcium uptake (44).

High sarcoplasmic energy demand, as observed in states of high cardiac output associated with acute stress as in fluid-resuscitated sepsis, will induce increases in

cytosolic calcium that are relayed by calcium transporters into the matrix, thereby raising mitochondrial calcium levels (45). Free intra-mitochondrial calcium activates pyruvate dehydrogenase, citric acid cycle dehydrogenases and ATP synthase, increasing reduction to NADH and stimulating ATP production (46, 47). This allows an extra level of fine regulation of energy homeostasis within the cell (48). In cardiomyocytes isolated from septic animals with good prognosis we observed that contraction-induced Rhod-2 levels increased more slowly, and to a lesser extent, than in sham controls. This can contribute to a lower activation of mitochondrial dehydrogenases, rending them less responsive to changes in calcium in response to increased ATP demand. This may explain the lower NADH peak to pacing in cardiomyocytes, and the lower kinetic energy release *in vivo* in response to dobutamine.

This observation may offer a protective effect. When mitochondrial calcium load exceeds the capacity of the NCX transporter (the main mechanism for calcium extrusion out of the mitochondria), mitochondria will start to accumulate calcium (49). If the buffering capacity is exceeded mitochondrial calcium concentration will rise leading to activation of the mPTP and consequent influx of water and small solutes, irreversible swelling, increased production of reactive oxygen species and eventual cell death (50). Mitochondrial swelling, decreased electron density and distorted cristae have been described in severe septic cardiomyopathy (15,29) as well as in autopsy studies in patients dying of septic shock (51). Intermyofibrillar mitochondria and jSR lie in close proximity, enabling mitochondria to sense acute changes in calcium released from the jSR (31). Our electron microscopy studies showed both a reduced area for

potential contacts (mitochondrial transversal side length) and an increased distance between organelles in septic hearts taken from good prognosis animals. This loss of proximity could be the explanation behind a lower mitochondrial calcium signal. Furthermore, in our selected population of animals with good prognosis we did not observed the structural changes in mitochondria described in more severe models.

Our work has limitations. First, our prediction of long-term survival in early sepsis is good but not perfect, however all the animals have similar genetic background, age, gender and upbringing, and all received the same dose of faecal slurry from a single batch. Second, since our cell experiments were only performed on good prognosis septic animals, we cannot be certain that mitochondrial calcium overload plays a role in mortality animals with bad prognosis. Third, despite Rhod2 being a sensitive marker of mitochondrial calcium (52), it is possible that mitochondria calcium measurements are contaminated by elevations in sarcoplasmic reticulum calcium with twitching. Fourth, the impact of low mitochondrial membrane potential in mitochondrial calcium uptake upon stimulation in septic cardiomyopathy should be further explored. Finally, the mitochondria-jSR architecture is regulated by numerous different proteins (e.g. mitofusin 2). Their role in septic cardiomyopathy remains to be fully elucidated.

Conclusions

To our knowledge, this is the first time that cardiac bioenergetics have been studied in septic animals with a distinct phenotype related to outcome, that supports the "hibernation" hypothesis in the context of septic cardiomyopathy. An increase in the distance that separates mitochondria from junctional sarcoplasmic reticulum could protect mitochondria from calcium overload in situations of high energetic demand, as observed in septic shock patients with high cardiac output states (53, 54), but at the cost of worsen systolic function.

References

1. Rabuel C, Mebazaa A: Septic shock: a heart story since the 1960s. *Intensive Care Med* 2006; 32:799-807

2. Zaky A, Deem S, Bendjelid K, et al: Characterization of cardiac dysfunction in sepsis: an ongoing challenge. *Shock* 2014; 41:12-24

3. Rudiger A, Singer M: Mechanisms of sepsis-induced cardiac dysfunction. *Crit Care Med* 2007; 35:1599-1608

4. Fenton KE, Parker MM: Cardiac Function and Dysfunction in Sepsis. *Clin Chest Med* 2016; 37:289-298

5. Singer M: The role of mitochondrial dysfunction in sepsis-induced multi-organ failure. *Virulence* 2014; 5:66-72

6. Carre JE, Orban JC, Re L, et al: Survival in critical illness is associated with early activation of mitochondrial biogenesis. *Am J Respir Crit Care Med* 2010; 182:745-751

7. Brealey D, Brand M, Hargreaves I, et al: Association between mitochondrial dysfunction and severity and outcome of septic shock. *Lancet* 2002; 360:219-223

8. Arulkumaran N, Deutschman CS, Pinsky MR, et al: Mitochondrial Function in Sepsis. *Shock* 2016; 45:271-281

9. McCreath G, Scullion MM, Lowes DA, et al: Pharmacological activation of endogenous protective pathways against oxidative stress under conditions of sepsis. *Br J Anaesth* 2016; 116:131-139

10. Rocheteau P, Chatre L, Briand D, et al: Sepsis induces long-term metabolic and mitochondrial muscle stem cell dysfunction amenable by mesenchymal stem cell therapy. *Nat Commun* 2015; 6:10145

11. Supinski GS, Callahan LA: Polyethylene glycol-superoxide dismutase prevents endotoxin-induced cardiac dysfunction. *Am J Respir Crit Care Med* 2006; 173:1240-1247

12. Supinski GS, Murphy MP, Callahan LA: MitoQ administration prevents endotoxin-induced cardiac dysfunction. *Am J Physiol Regul Integr Comp Physiol* 2009; 297:R1095-1102

13. Hotchkiss RS, Song SK, Neil JJ, et al: Sepsis does not impair tricarboxylic acid cycle in the heart. *Am J Physiol* 1991; 260:C50-57

14. McDonough KH, Henry JJ, Lang CH, et al: Substrate utilization and high energy phosphate levels of hearts from hyperdynamic septic rats. *Circulatory shock* 1986; 18:161-170

15. Watts JA, Kline JA, Thornton LR, et al: Metabolic dysfunction and depletion of mitochondria in hearts of septic rats. *J Mol Cell Cardiol* 2004; 36:141-150

16. Starling EH, Visscher MB: The regulation of the energy output of the heart. *J Physiol* 1927; 62:243-261

17. Brand MD, Nicholls DG: Assessing mitochondrial dysfunction in cells. *Biochem J* 2011; 435:297-312

18. Griffiths EJ, Rutter GA: Mitochondrial calcium as a key regulator of mitochondrial ATP production in mammalian cells. *Biochim Biophys Acta* 2009; 1787:1324-1333

19. McCormack JG, Denton RM: Intracellular calcium ions and intramitochondrial Ca2+ in the regulation of energy metabolism in mammalian tissues. *Proc Nutr Soc* 1990; 49:57-75

20. Davidson SM, Derek MY, Murphy MP, et al: Slow calcium waves and redox changes precede mitochondrial permeability transition pore opening in the intact heart during hypoxia and reoxygenation. *Cardiovascular Research* 2012; 93:445–453

21. Vieillard Baron A, Schmitt JM, Beauchet A, et al: Early preload adaptation in septic shock? A transesophageal echocardiographic study. *Anesthesiology* 2001; 94:400-406

22. Vieillard-Baron A, Prin S, Chergui K, et al: Hemodynamic instability in sepsis: bedside assessment by Doppler echocardiography. *Am J Respir Crit Care Med* 2003; 168:1270-1276

23. Weng L, Liu YT, Du B, et al: The prognostic value of left ventricular systolic function measured by tissue Doppler imaging in septic shock. *Crit Care* 2012; 16:R71

24. Landesberg G, Gilon D, Meroz Y, et al: Diastolic dysfunction and mortality in severe sepsis and septic shock. *Eur Heart J* 2012; 33:895-903

25. Chang W-T, Lee W-H, Lee W-T, et al: Left ventricular global longitudinal strain is independently associated with mortality in septic shock patients. *Intensive Care Med*; 2015:1791-1799

26. Masson S, Caironi P, Fanizza C, et al: Sequential N-Terminal Pro-B-Type Natriuretic Peptide and High-Sensitivity Cardiac Troponin Measurements During Albumin Replacement in Patients With Severe Sepsis or Septic Shock. *Crit Care Med* 2016; 44:707-716

27. Wang F, Wu Y, Tang L, et al: Brain natriuretic peptide for prediction of mortality in patients with sepsis: a systematic review and meta-analysis. *Crit Care* 2012; 16:R74

28. Bessiere F, Khenifer S, Dubourg J, et al: Prognostic value of troponins in sepsis: a meta-analysis. *Intensive Care Med* 2013; 39:1181-1189

29. Rudiger A, Dyson A, Felsmann K, et al: Early functional and transcriptomic changes in the myocardium predict outcome in a long-term rat model of sepsis. *Clinical Science;* 2013; 124: 391–401

30. Zolfaghari P, Pinto BB, Dyson A, et al: The metabolic phenotype of rodent sepsis: cause for concern? *Intensive Care Med Exp* 2013; 1:25

31. Chen Y, Csordas G, Jowdy C, et al: Mitofusin 2-Containing Mitochondrial-Reticular Microdomains Direct Rapid Cardiomyocyte Bioenergetic Responses via Inter-Organelle Ca2+ Crosstalk. *Circ Res* 2012; 111:863-875

32. Gonnert FA, Recknagel P, Seidel M, et al: Characteristics of clinical sepsis reflected in a reliable and reproducible rodent sepsis model. *J Surg Res* 2011; 170:e123-134.

33. Brealey D, Karyampudi S, Jacques TS, et al: Mitochondrial dysfunction in a long-term rodent model of sepsis and organ failure. *Am J Physiol Regul Integr Comp Physiol* 2004; 286:R491-497

34. Slama M, Susic D, Varagic J, et al: Echocardiographic measurement of cardiac output in rats. *Am J Physiol Heart Circ Physiol* 2003; 284:H691-697

35. Dowell RT, Houdi AA: Aortic peak flow velocity as an index of myocardial contractility in the conscious rat. *Methods Find Exp Clin Pharmacol* 1997; 19:533-539

36. Atlas G, Brealey D, Dhar S, et al: Additional hemodynamic measurements with an esophageal Doppler monitor: a preliminary report of compliance, force, kinetic energy, and afterload in the clinical setting. *J Clin Monit Comput* 2012; 26:473-482

37. Maddock HL, Mocanu MM, Yellon DM: Adenosine A(3) receptor activation protects the myocardium from reperfusion/reoxygenation injury. *Am J Physiol Heart Circ Physiol* 2002; 283:H1307-1313

38. Davidson SM, Hausenloy D, Duchen MR, et al: Signalling via the reperfusion injury signalling kinase (RISK) pathway links closure of the mitochondrial permeability transition pore to cardioprotection. *Int J Biochem Cell Biol* 2006; 38:414-419

39. Leyssens A, Nowicky AV, Patterson L, et al: The relationship between mitochondrial state, ATP hydrolysis, [Mg2+]i and [Ca2+]i studied in isolated rat cardiomyocytes. *J Physiol* 1996; 496:111-128

40. Griffiths EJ: Species dependence of mitochondrial calcium transients during excitation-contraction coupling in isolated cardiomyocytes. *Biochem Biophys* 1999; 263:554–559

41. Rudiger A, Singer M: The heart in sepsis: from basic mechanisms to clinical management. *Curr Vasc Pharmacol* 2013; 11:187-195

42. Chopra M, Golden HB, Mullapudi S, et al: Modulation of myocardial mitochondrial mechanisms during severe polymicrobial sepsis in the rat. *PloS One* 2011; 6:e21285

43. Lancel S, Joulin O, Favory R, et al: Ventricular myocyte caspases are directly responsible for endotoxin-induced cardiac dysfunction. *Circulation* 2005; 111:2596-2604

44. Finkel T, Menazza S, Holmström KM, et al: The Ins and Outs of Mitochondrial Calcium. *Circulation Res* 2015; 116: 1810-1919

45. Bell CJ, Bright NA, Rutter GA, et al: ATP regulation in adult rat cardiomyocytes: time-resolved decoding of rapid mitochondrial calcium spiking imaged with targeted photoproteins. *J Biol Chem* 2006; 281:28058-28067

46. Jouaville LS, Pinton P, Bastianutto C, et al: Regulation of mitochondrial ATP synthesis by calcium: evidence for a long-term metabolic priming. *Proc Natl Acad Sci U S A* 1999; 96:13807-13812

47. McCormack JG, Halestrap AP, Denton RM: Role of calcium ions in regulation of mammalian intramitochondrial metabolism. Physiol Rev 1990; 70:391-425

48. Winslow RL, Walker MA, Greenstein JL: Modeling calcium regulation of contraction, energetics, signaling, and transcription in the cardiac myocyte. *Wiley Interdiscip Rev Syst Biol Med* 2016; 8:37-67

49. Szabadkai G, Duchen MR: Mitochondria: the hub of cellular Ca2+ signaling. *Physiology (Bethesda)* 2008; 23:84-94

50. Yarana C, Sripetchwandee J, Sanit J, et al: Calcium-induced cardiac mitochondrial dysfunction is predominantly mediated by cyclosporine A-dependent mitochondrial permeability transition pore. *Arch Med Res* 2012; 43:333-8

51. Rossi MA, Celes MR, Prado CM, Saggioro FP: Myocardial structural changes in long-term human severe sepsis/septic shock may be responsible for cardiac dysfunction. *Shock* 2007; 27:10-18

52. Davidson SM, Yellon D, Duchen MR: Assessing mitochondrial potential, calcium, and redox state in isolated mammalian cells using confocal microscopy. *Methods Mol Biol* 2007; 372:421-430

53. Parker MM, Shelhamer JH, Natanson C, et al: Serial cardiovascular variables in survivors and nonsurvivors of human septic shock: heart rate as an early predictor of prognosis. *Crit Care Med* 1987; 15:923-929

54. Kumar A, Schupp E, Bunnell E, et al: Cardiovascular response to dobutamine stress predicts outcome in severe sepsis and septic shock. *Crit Care* 2008; 12:R35

Figure legends

Figure 1 – Kaplan-Meier survival curve.

Median survival in the sepsis group was 49 hours. p=0.0255 (Log-rank test).

Figure 2 – Effects of changes in metabolic demand (pacing) on mitochondrial calcium and bioenergetic intermediates in cardiomyocytes detected by confocal microscopy.

(A) Cardiomyocytes loaded with TMRM 15nM were sequentially excited with UV (350nm) and HeNe (543nm) lasers to image NADH autofluorescence (peak emission 450 nm, reporter of mitochondrial redox state) and TMRM fluorescence (peak emission 577nm, reporter of mitochondrial membrane potential). Co-localisation of the NADH and TMRM signals can be seen in the longitudinally distributed mitochondria. Addition of the mitochondrial uncoupler FCCP caused fast decay of both signals due to membrane depolarisation and oxidation of the NADH pool (data not shown). (B) Quantification of the mean NADH and TMRM signals at rest. (C) Cardiomyocytes loaded with Rhod-2AM 5 μM were excited at 552nm for mitochondrial calcium imaging. After basal measurements, field stimulation at 3 Hz was performed. (D) Cardiomyocytes loaded with Fluo-4AM 5 μM were excited at 488nm for total calcium imaging. After basal measurements, field stimulation at 3 Hz was performed. (E) Cardiomyocytes loaded with MgGreen AM 5 μM were excited with an Argon laser at 488nm and imaged every 3 seconds. (F) Cardiomyocytes excited with a UV (351nm) laser to image NADH autofluorescence. After basal measurements, field stimulation at 3 Hz was performed. The peak rise in NADH autofluorescence was higher in sham cardiomyocytes (§ - p=0.01046, for 2-way Repeated Measures ANOVA, and *p<0.05

for post-hoc Bonferroni correction at individual time points). Legend: 2-DEO – 2-deoxyglucose (20nM); a.u. – arbitrary units, FCCP - Carbonyl cyanide 4-(trifluoromethoxy)phenylhydrazon (0.4µM); Oligomycin (2.5 µg/ml), * $p<0.05$ vs. sham, ** $p<0.01$ vs. sham, § for two-way ANOVA. Data shown as mean±SEM.

Figure 3 – Mitochondria–junctional sarcoplasmic reticulum contacts.

Representative electron micrographs of myocardium sections retrieved from sham (A) and sepsis good-prognosis (B) animals, showing intermyofibrillar mitochondria (m), t-tubules (t) and lining jSR (*), and quantification of mitochondrial-jSR contacts: mitochondrial transversal side length (C), mitochondrial transversal side contact with jSR (D), and mitochondrial outer membrane to jSR gap length (E). Data are shown as mean ± SEM. p-value is for Mann Whitney test. Legend: * $p<0.05$ vs. sham; jSR – junctional sarcoplasmic reticulum; OMM – outer mitochondrial membrane.

Figure 4 – Effect of a dobutamine challenge on echocardiography-derived measures of cardiac function at 6 and 24 h post-insult.

Dobutamine was increased at 5-minute intervals from 2.5 to 10 µg/kg/min. ΔSV (stroke volume) and ΔKE (kinetic energy) represent the difference between values at 10 µg/kg/min and baseline. Legend: * $p<0.05$ vs. sham; ** $p<0.01$ vs. sham.

Table legend:

Table 1 – Echocardiography-derived parameters of cardiac function at 6, 24 and 72 h post-insult.

The p-value shown is for one-way ANOVA analysis of variance within each time-point, with post-hoc Bonferroni correction (a, b).

a – p<0.05 vs. sham; b - p<0.05 vs. sepsis survivors; bpm – beats per minute; CO – cardiac output; HR – heart rate; KE – kinetic energy; m/s – meters per second; ns – non-significant; PVel – peak velocity; SV – stroke volume.

Variable	Time	sham	sepsis survivors	sepsis non-survivors	p-value
PV (m/s)	6h	0.93±0.06	0.86±0.05	0.80±0.03	ns
	24h	0.95±0.05	0.94±0.04	0.58±0.1[a,b]	0.004
	72h	1.02±0.06	0.97±0.06	-	ns
SV (ml)	6h	0.24±0.02	0.22±0.01	0.18±0.01[a]	0.004
	24h	0.23±0.01	0.23±0.02	0.13±0.03[a,b]	0.004
	72h	0.27±0.02	0.26±0.02	-	ns
HR (bpm)	6h	420±16	446±14	478±12[a]	0.02
	24h	398±11	435±14	403±44	ns
	72h	387±11	396±17	-	ns
CO (ml/min)	6h	100±6	97±4	86±3	0.049
	24h	93±4	97±5	55±16[a,b]	0.006
	72h	103±6	100±4	-	ns
KE (mjoules)	6h	121±21	92±17	64±6[a]	0.03
	24h	117±17	91±14	43±21[a]	0.03
	72h	154±25	134±16	-	ns

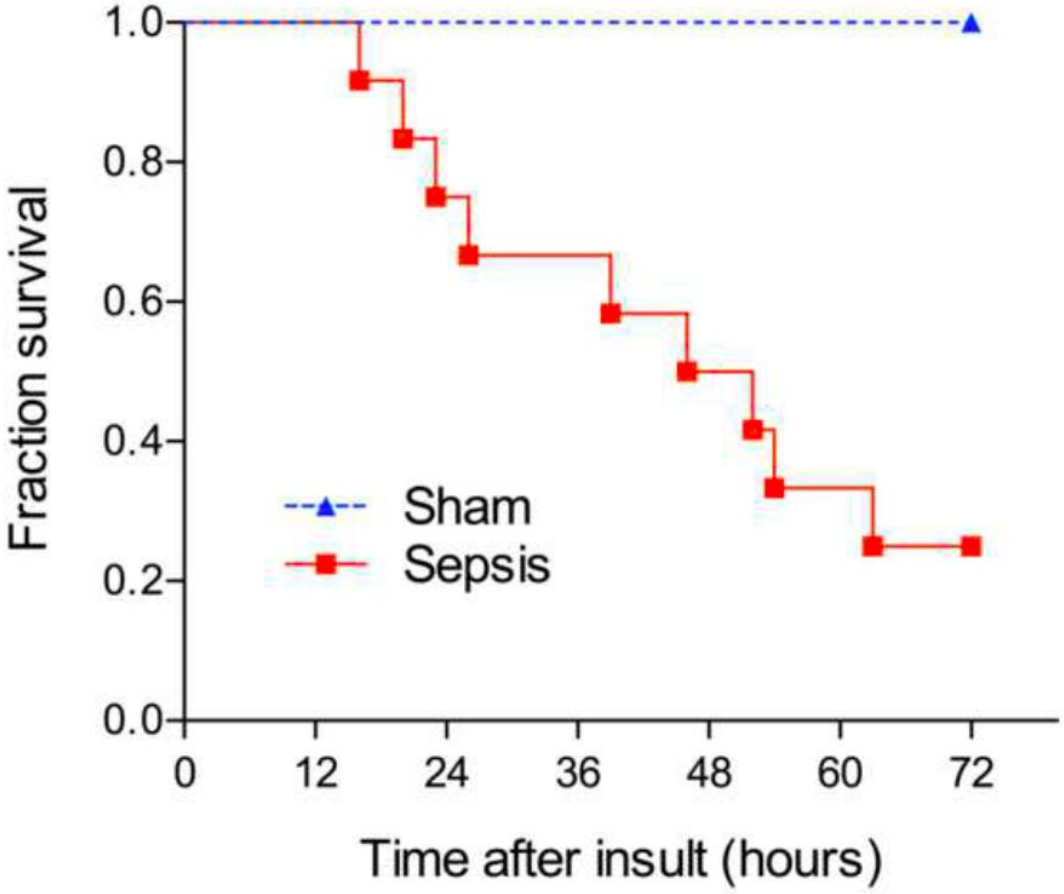
1.0
0.8
0.6
0.4
0.2
0.0
Fraction survival
Sham
Sepsis
0
12
24
36
48
60
72
Time after insult (hours)

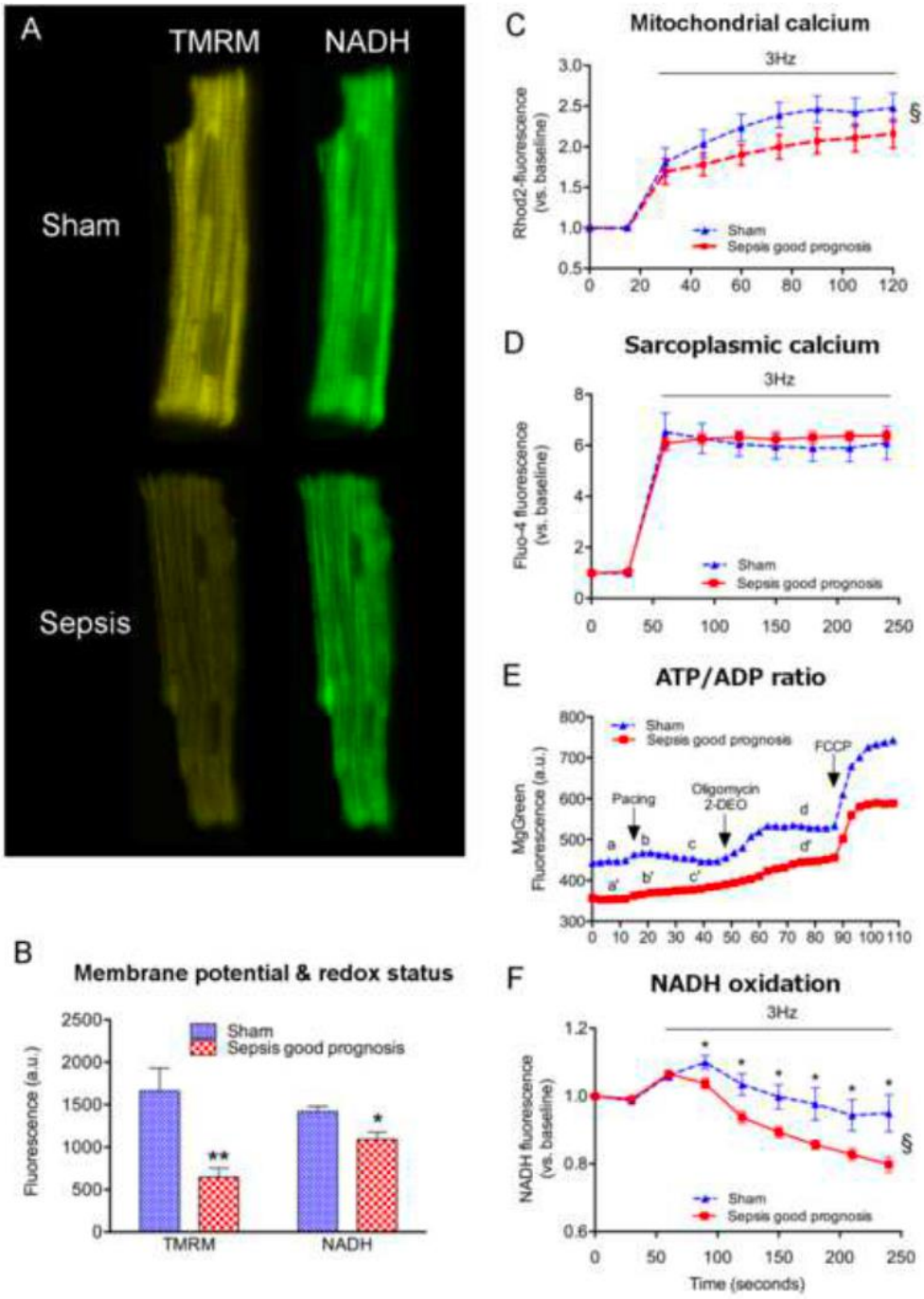
A
TMRM
NADH
Sham
Sepsis
B
Membrane potential & redox status
Fluorescence (a.u.)
Sham
Sepsis good prognosis
TMRM
NADH
C
Mitochondrial calcium
3Hz
Rhod2-fluorescence (vs. baseline)
Sham
Sepsis good prognosis
Time (seconds)
D
Sarcoplasmic calcium
3Hz
Fluo-4 fluorescence (vs. baseline)
Sham
Sepsis good prognosis
Time (seconds)
E
ATP/ADP ratio
MgGreen Fluorescence (a.u.)
Sham
Sepsis good prognosis
Pacing
Oligomycin 2-DEO
FCCP
Time (seconds)
F
NADH oxidation
3Hz
NADH fluorescence (vs. baseline)
Sham
Sepsis good prognosis
Time (seconds)

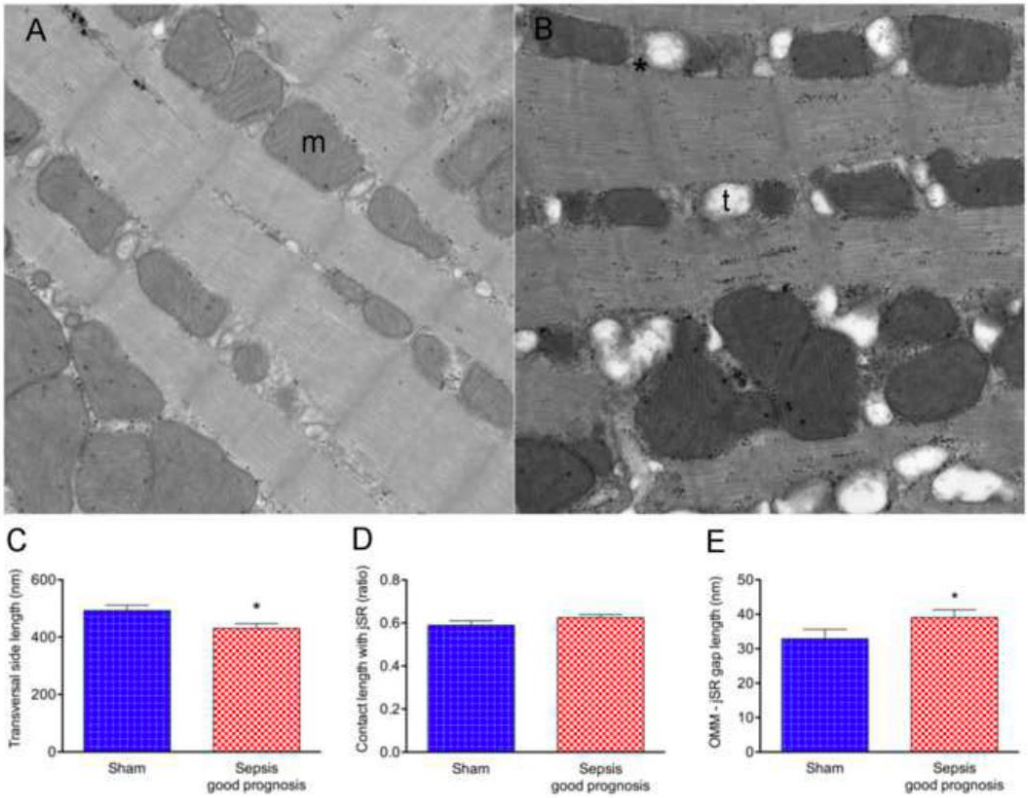
A
m
B
*
t
C
Transversal side length (nm)
600
400
200
0
*
Sham
Sepsis
good prognosis
D
Contact length with jSR (ratio)
0.8
0.6
0.4
0.2
0.0
Sham
Sepsis
good prognosis
E
OMM - jSR gap length (nm)
50
40
30
20
10
0
*
Sham
Sepsis
good prognosis

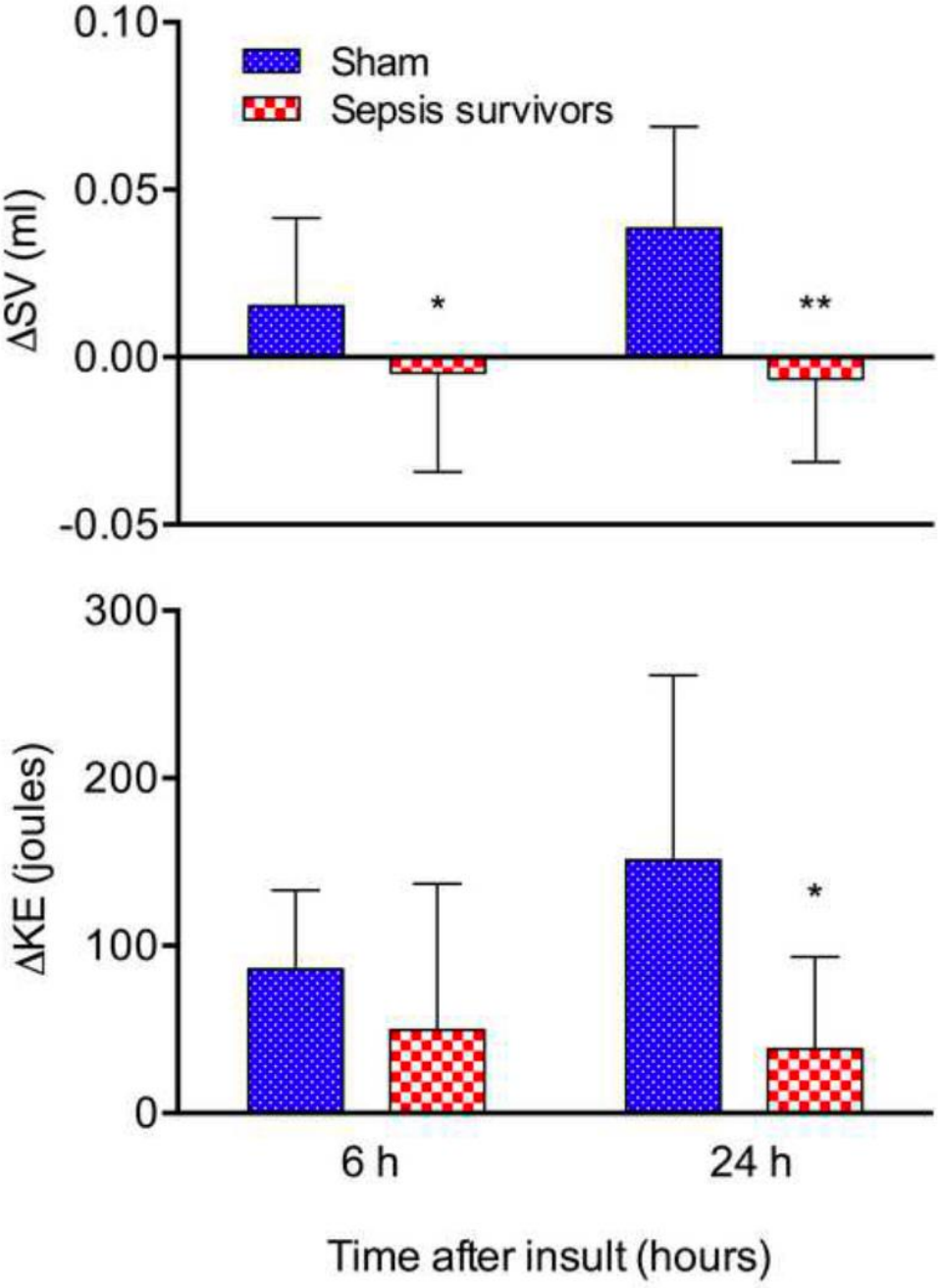
0.10
0.05
0.00
-0.05
ΔSV (ml)
Sham
Sepsis survivors
*
**
300
200
100
0
ΔKE (joules)
*
6 h
24 h
Time after insult (hours)

Supplemental Digital Content legend

Supplemental Digital Content 1 – Study cohorts

Mortality and clinical severity score of all study cohorts.

Supplemental Digital Content 2 – Methodology

Additional methodology information on rat model, echocardiography measurements, isolation of cardiomyocytes, confocal microscopy settings and electron microscopy measurements.

Supplemental Digital Content 3 – Characterization of cohort 1

Clinical severity score, blood pressure and biochemical parameters of disease.

Supplemental Digital Content 4 – Receiver operating curves for prediction of 72 h survival

Supplemental Digital Content 5 – Quantitative parameters of mitochondria density, size and shape.